Pressure study of the magnetic and electrical properties of the Eu-Yb alloy system

H. Kadomatsu, T. Tsutaoka, and H. Fujiwara
Faculty of Science, Hiroshima University, 1-1-89 Higashisenda, Hiroshima 730, Japan
(Received 25 February 1985)

Measurements of the ac magnetic susceptibility, magnetization, and electrical resistivity at hydrostatic pressures up to 15 kbar and of the thermal expansion were made for the Eu_xYb_{1-x} alloy system ($x \leq 0.4$) in temperatures from 1.6 to 400 K. The paramagnetic-ferromagnetic transition temperature T_c versus pressure p curve for $x=0.025$ has a maximum near $p=1$ kbar. For $x=0.25$, T_c decreases and the ferromagnetic—spin-glass-like transition temperature T_t increases at rates of $\Delta T_c/\Delta p=-9.5$ K/kbar and $\Delta T_t/\Delta p=+1.7$ K/kbar, respectively. The ferromagnetic region disappears near $p=2.5$ kbar, and above it the paramagnetic—spin-glass-like transition temperature T_g, which is pressure insensitive, appears. The T_g value for $x=0.35$ decreases initially and increases slowly with increasing p above $p=2$ kbar at a rate of $\Delta T_g/\Delta p=+0.15$ K/kbar. Both the magnetization in the ferromagnetic concentration range and the value of the ac magnetic susceptibility near T_g in the spin-glass-like state decrease with increasing p. From electrical-resistivity measurements under various pressures, semiconducting character was observed at the ambient pressure for $x=0.35$ and the transition from semimetallic to semiconducting states appears with increasing p for $x=0.025$. Thermal expansion shows the large positive volume magnetostriction. These results of the measurements under pressure are discussed on the basis of the Ruderman-Kittel-Kasuya-Yosida interaction by considering that the dominant variable is the number of carriers (electrons or holes) which is strongly controlled by the pressure.

I. INTRODUCTION

In rare-earth metals and alloys, it has been generally accepted that the exchange interaction for producing the magnetic ordering is the indirect one [the Ruderman-Kittel-Kasuya-Yosida (RKKY) interaction],[1,2] in which the electrons in the $5d\,6s$ conduction band are responsible for the interactions between the well-localized moments of the $4f$ magnetic electrons. With respect to this interaction, therefore, the properties of the $5d\,6s$ band, such as the number of carriers, the density of states at the Fermi level, etc., are important factors to be considered. In order to understand the role of these factors and/or the mechanism of the exchange interaction from the experimental point of view, the substitution method has been usually employed, in which the matrix element is substituted by an element with a different number of valence electrons from that of the matrix; thus the number of $5d\,6s$ band electrons could be changed.[3] The results obtained from this method (alloying effect), however, cannot be analyzed simply as a function only of the number of band electrons, since the alloying effect might be accompanied by so-called spatial heterogeneity or randomness of the electronic structure, for example.

On the other hand, hydrostatic pressure deforms the $5d\,6s$ band uniformly and pressure has been considered a clean technique in this respect. For the purpose of investigating the effect of pressure on the exchange interaction, the variation of the magnetic transition temperature with pressure is the most straightforwardly observable quantity. The effect of pressure on the magnetic transition temperature through the deformation of the $5d\,6s$ band is about 1 K/kbar for the metallic alloys and compounds in which the constituent elements are rare earths.[4] Therefore, if we choose a system in which the number of conduction electrons could also be controlled by the application of pressure, the change induced in the magnetic properties will be drastically enhanced, and we will obtain more information about the mechanism of the indirect exchange interaction than can be found in the stable system. In the present work, the Yb-rich Eu-Yb alloy system Eu_xYb_{1-x} was chosen as an appropriate one with respect to the above-mentioned circumstances for the following reasons. (i) The crystal structure of the system for $x<0.5$ is a simple fcc.[5] (ii) The electrical character of pure Yb changes from semimetallic to semiconducting with application of pressure.[6–8] Therefore, the number of conduction electrons is expected to be controlled with pressure in Yb-rich alloys. (iii) Since an Eu atom has the electronic structure for the divalent and $^8S_{7/2}$ ground states, it is not necessary to consider the magnetic anisotropy which comes from the orbital effect. Therefore, the data obtained from polycrystalline samples are sufficient.

In the course of our investigation, we first studied the magnetic and electrical properties at ambient pressure. The concentration x versus temperature T magnetic phase diagram[9] obtained is shown in Fig. 1(a) (Fig. 3 in Ref. 9), where we have found the paramagnetic (PARA), ferromagnetic (FERRO), and spin-glass-like (SG) phases. The transition from semimetallic (SM) to semiconducting (SC) states appears near $x \simeq 0.1$, as indicated in Fig. 1(b). Secondly, with the same sample that was used for establishing the phase diagram, we measured the effects of hydrostatic pressure on the paramagnetic-ferromagnetic transition temperature T_c, the ferromagnetic—spin-glass-like transition temperature T_t, the paramagnetic—spin-

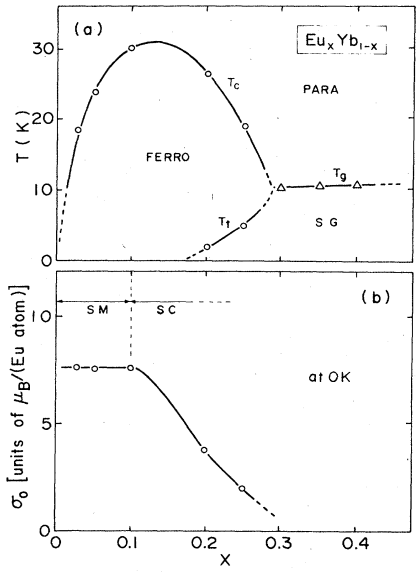

FIG. 1. (a) Concentration x vs temperature T magnetic phase diagram and (b) spontaneous magnetization at 0 K, σ_0 vs x curve. In (b) the semimetallic (SM) and semiconducting (SC) ranges also are shown. They are quoted from Ref. 9.

glass-like transition temperature T_g, the magnetization σ, and the electrical resistivity ρ. The thermal expansion was also measured. The results obtained have revealed the remarkable positive volume magnetostriction effect and have already been briefly reported.[10,11] This paper is concerned with the summary of our results obtained so far in order to understand how the pressure-induced change in the number of conduction electrons modifies the magnetism; that is, the magnetic phase diagram.

II. EXPERIMENTAL PROCEDURES

The concentrations of 99.9% pure Eu and 99.9% pure Yb were sealed in a tantalum crucible in an Ar atmosphere, melted at 1000 °C in an electric furnace, and the alloys were obtained after rapid cooling. Subsequent annealing in order to homogenize the composition was done at 500 °C for one week. The Eu concentrations x in the prepared samples were $x=0.025$, 0.05, 0.1, 0.2, 0.25, 0.3, 0.35, and 0.4. With x-ray diffraction, it was confirmed that the crystal structure of all the samples thus prepared was fcc at room temperature.

The samples were shaped into spheres of ~ 3—4 mm in diameter for the ac magnetic susceptibility and magnetization measurements, and into rectangular rods of $0.5\times1\times2$ mm^3 for the electrical resistivity measurement. They were $1\times1\times5$ mm^3 for the thermal expansion measurement. After shaping, the annealing for removing the strain was done at 500 °C for several hours. The ac magnetic susceptibility was measured with a Hartshorn bridge circuit at weak magnetic field of amplitude 1 Oe and frequency 800 Hz. The magnetization was measured with an induction method in magnetic fields up to 20 kOe. The electrical resistivity was measured by a standard four-probe dc method with a nanovoltmeter. The thermal expansion was measured with a differential-transformer-type dilatometer.

High hydrostatic pressures were generated in the clamp-type piston (WC) —cylinder (Be-Cu) pressure cell[12] for the electrical resistivity and susceptibility measurements and in the clamp-type piston (Al_2O_3)—cylinder (Be-Cu) miniature pressure cell[13] for the magnetization measurement. The sample was set in a Teflon bucket in the cell and the bucket was filled up with mixture of 1:1 n-pentane and isoamyl alcohol as the pressure-transmitting medium. Pressurization was always done at room temperature. Pressure values at room temperature, 4.2 K, and those between room temperature and 4.2 K were determined with the crystallographic transition pressure of NH_4F, the pressure dependence of the superconducting transition temperature of Sn, and the pressure dependence of the resistance of manganin wire,[12] respectively.

The temperature was determined with a AuFe-Chromel thermocouple and a carbon and Ge thermometer. Magnetic fields up to 20 kOe were generated by a laboratory electromagnet.

III. EXPERIMENTAL RESULTS

A. Magnetic and electrical properties at ambient pressure

Before describing the data obtained at high pressures, the results obtained at ambient pressure in Ref. 9 will be briefly summarized by using the data shown in Figs. 1(a) and 1(b). The x-T magnetic phase diagram in the figure is composed of three phases: paramagnetic (PARA), ferromagnetic (FERRO), and spin-glass-like (SG) phases. In the range from $x=0.2$ to 0.3, the phase transitions from the paramagnetic to the ferromagnetic and from the ferromagnetic to the spin-glass-like states develop successively with decreasing temperature. With respect to the spin-glass-like phase, Legvold and Beaver[14] did not observe the boundary temperature T_g, which has been found in the present work, and the reason for this inconsistency will be understood from the following experiments. In the temperature dependence of the ac magnetic susceptibility χ, a sharp maximum was observed at T_g. When a dc magnetic field was applied, however, the χ value at T_g and T_g itself decreased rapidly with increasing dc magnetic field, suggesting the sensitivity of χ for the dc field. Legvold and Beaver measured χ in the relatively high-field range, so that it was possible that they could not find the transition temperature T_g. As seen in Fig. 1(b), the spontaneous magnetization at 0 K, σ_0, obtained from the back extrapolation of the temperature dependence of magnetization, is $7.6\mu_B$/(Eu atom) for $x\leq0.1$. This value is larger than the theoretical value $gJ=7\mu_B$ and the excess magnetic moment $0.6\mu_B$ may come from the $5d6s$ polarization. For $x>0.1$, σ_0 decreases with increasing x.

With respect to the electrical properties, the alloys had semimetallic ($\Delta\rho/\Delta T>0$) and semiconducting ($\Delta\rho/\Delta T<0$) characters for $x<0.1$ and $x>0.1$, respectively. The lattice constant of the alloy system increases

with increasing x and may be linearly interpolated between the lattice constant of pure Yb and the calculated constant for the fictitious fcc Eu. Therefore the transition to the semiconducting state due to an increase in x may suggest that the fictitious fcc Eu is either a semiconductor or an insulator. The anomaly in ρ was observed at T_c but not at T_t or T_g.

B. Pressure effect on the magnetic transition temperatures T_c, T_t, and T_g

The results of the pressure dependences of the magnetic transition temperatures T_c, T_t, and T_g obtained from the χ measurements will be given separately for respective alloy samples.

(i) $Eu_{0.025}Yb_{0.975}$ ($x=0.025$). This is the most dilute alloy sample in the present work; one Eu atom exists on an average in the third-nearest-neighbor sphere of Yb. Figure 2(a) gives the χ versus T curves at various pressures p and the T_c versus p curve obtained from Fig. 2(a) is plotted in Fig. 2(b). The T_c value is defined as an inflection point[15,16] in the χ versus T curve as indicated by an arrow shown in Fig. 2(a), where χ increases abruptly with lowering temperature. It is to be mentioned that the relative magnitude of χ below T_c decreased drastically with increasing p. In Fig. 2(b) the T_c value increases initially at a rate of $\Delta T_c/\Delta p \simeq +2$ K/kbar, reaches a maximum around $p=1.5$ kbar, and decreases in an S-shape curve and the ferromagnetic phase appears to vanish around $p=7$ kbar, with increasing p.

(ii) $Eu_{0.10}Yb_{0.90}$ ($x=0.10$). This sample has the highest T_c value of the present samples. In Figs. 3(a) and 3(b) are shown the χ versus T curves for various p and the T_c versus p curve obtained from Fig. 3(a), respectively. The value of T_c decreases almost linearly at a rate of $\Delta T_c/\Delta p = -6.0$ K/kbar and appears to vanish around $p=5$ kbar.

(iii) $Eu_{0.20}Yb_{0.80}$ ($x=0.20$). This sample shows the

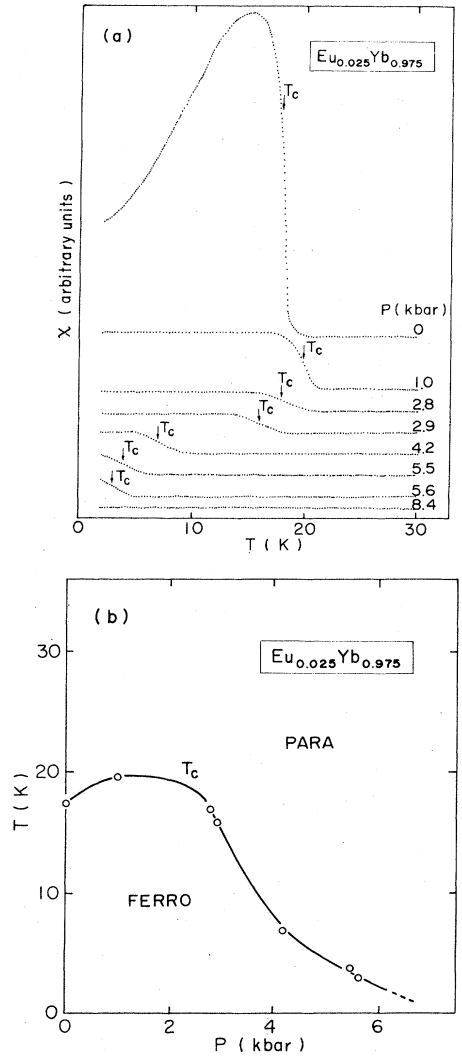

FIG. 2. (a) ac magnetic susceptibility χ vs temperature T at various pressures p and (b) magnetic transition temperature T_c vs p curve. Sample is $Eu_{0.025}Yb_{0.975}$.

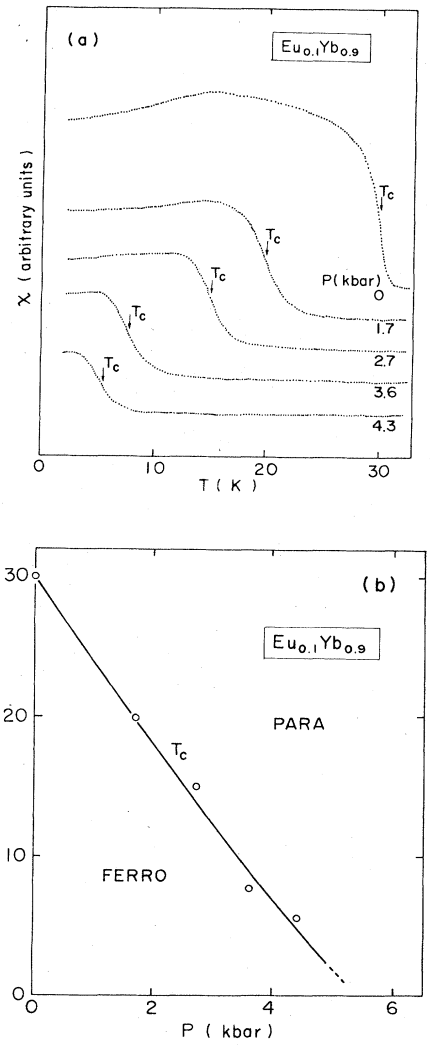

FIG. 3. (a) ac magnetic susceptibility χ vs temperature T curves at various pressures p and (b) T_c vs p curve. Sample is $Eu_{0.10}Yb_{0.90}$.

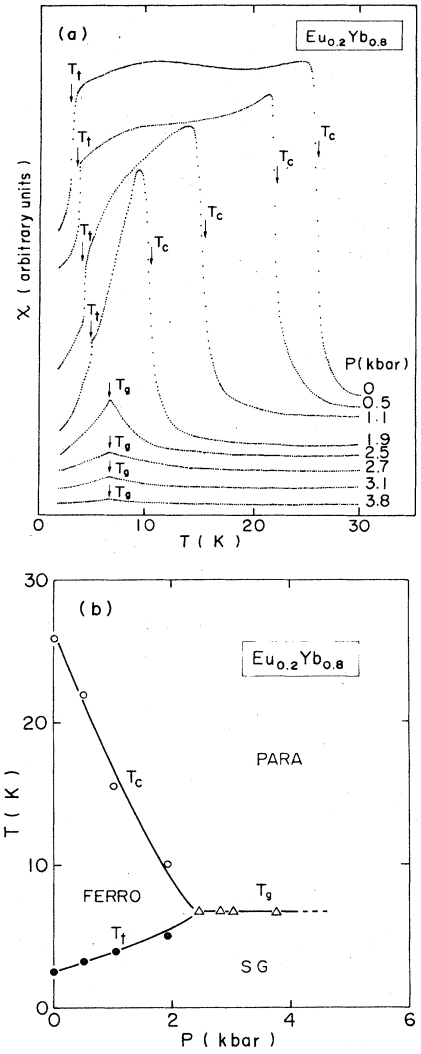

FIG. 4. (a) ac magnetic susceptibility χ vs temperature T curves at various pressures p and (b) magnetic transition temperatures T_c, T_t, and T_g vs p curves. Sample is $Eu_{0.20}Yb_{0.80}$.

most peculiar characteristics of the present work. Figure 4(a) shows the χ versus T curves at various p. At $p=0$ kbar, χ increases, with decreasing temperature, very steeply around 26 K ($=T_c$); its value is then almost constant below T_c. Then it decreases drastically around 2 K, which indicates the transition from a ferromagnetic to a spin-glass-like phase. The transition temperature T_t, defined also as an inflection point indicated by an arrow in the temperature-decreasing run, was found to be 2.3 K. As pressure increases, T_c decreases and T_t increases. The pressure derivatives of T_c and T_t, $\Delta T_c/\Delta p$ and $\Delta T_t/\Delta p$, were -9.5 K/kbar and $+1.7$ K/kbar, respectively. As far as we know, this value of $\Delta T_c/\Delta p$ is the largest in the alloy system composed of only rare-earth elements. The absolute value of the average slope of χ with temperature, $\Delta\chi/\Delta T$, in the ferromagnetic temperature range increases with increasing p.

It should be pointed out in Fig. 4(a) that the χ versus T curves show sharp cusps above a pressure of 1.9 kbar. From the analogy between the x-T magnetic phase diagram in Fig. 1(a) and the p-T magnetic phase diagram in Fig. 4(b) (Fig. 2 in Ref. 11), we have regarded the cusp point as T_g. The T_g value is almost pressure independent, which is very different from $\Delta T_c/\Delta p$ mentioned above. Above $p=4$ kbar, the anomaly in the χ versus T curve which represents T_g could not be detected, possibly due to the lack of the sensitivity of the χ measurement.

(iv) $Eu_{0.30}Yb_{0.70}$ ($x=0.30$). As is evident from Fig. 1(a), the ferromagnetism disappears or appears at concentration x close to 0.3. In the χ versus T curves in Fig. 5(a), only the transition temperature T_g has been observed. At $p=0$ kbar, the curve has a sharp peak although it is asymmetric and the curvature above T_g is concave downwards. As pressure increases, T_g decreases with an initial slope $\Delta T_g/\Delta p$ of -1.7 K/kbar and the slope becomes small at high pressure, as seen in Fig. 5(b). The χ values at T_g decrease rapidly with increasing p.

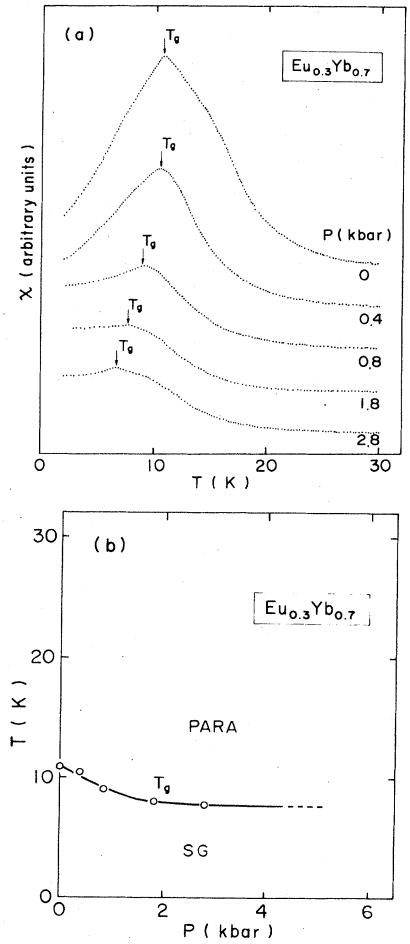

FIG. 5. (a) ac magnetic susceptibility χ vs temperature T curves at various pressures p and (b) T_g vs p curve. Sample is $Eu_{0.30}Yb_{0.70}$.

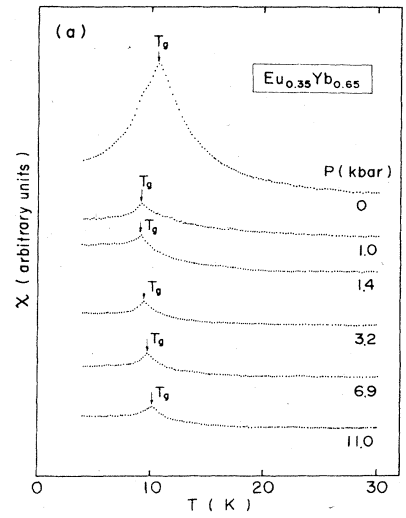

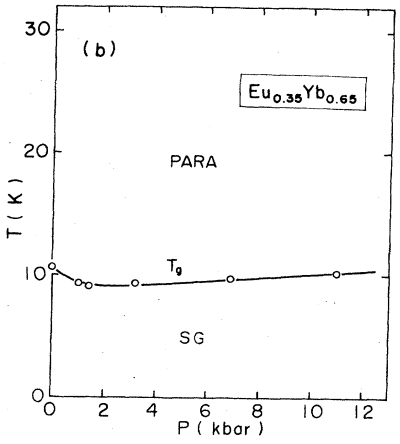

FIG. 6. (a) ac magnetic susceptibility χ vs temperature T curves at various pressures p and (b) T_g vs p curve. Sample is $Eu_{0.35}Yb_{0.65}$.

(v) $Eu_{0.35}Yb_{0.65}$ ($x=0.35$). Like the alloy with $x=0.30$, this alloy has only transition temperature T_g and T_g decreases with an initial slope of $\Delta T_g/\Delta p=-1.0$ K/kbar [Fig. 6(b)]. But T_g reaches a minimum around $p=2$ kbar and then increases definitely with increasing pressure, although the rate of increase is small, $\Delta T_g/\Delta p=+0.15$ K/kbar. Judging from this fact, the T_g value for $x=0.30$ shown in Fig. 5(b) also may increase with increasing p in the higher pressure range. In regard to the alloys with $x=0.30$ and 0.35, the summarized results are the following: (a) The magnitude of $\Delta T_g/\Delta p$ is very small in comparison with that of $\Delta T_c/\Delta p$ for the alloys with $x<0.30$, and (b) χ values at T_g drastically decrease with increasing pressure [Figs. 5(a) and 6(a)].

From the above-mentioned results of the pressure effects on T_c, T_t, and T_g, we can draw the three-dimensional temperature T-x-p magnetic phase diagram, and it is shown in Fig. 7.

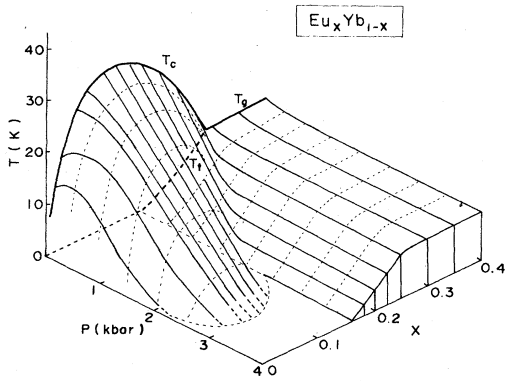

FIG. 7. Three-dimensional temperature T vs concentration x vs pressure p magnetic phase diagram.

C. Pressure effect on the magnetization

The pressure dependences of the magnetization were measured at 4.2 K. Figure 8 gives the magnetization σ versus the effective magnetic field H curves at various pressures for $x=0.025$, and the spontaneous magnetization σ_s versus p curve is shown in the inset. Here, σ is the magnetization per Eu atom in units of μ_B, and σ_s was obtained from Arrott's plot. Figures 9 and 10 are the results for $x=0.1$ and 0.2, respectively, and Fig. 11 concerns the magnetization curves for $x=0.35$. The points which should be mentioned in these figures are as follows. (a) The high-field susceptibility $\partial M/\partial H$ at $p=0$ kbar increases with increasing x. (b) For $x=0.025$ and 0.1, $\partial M/\partial H$ increases with increasing p. For $x=0.2$, the σ_s versus H curves at high field are almost parallel to each other; that is, the $\partial M/\partial H$'s are roughly pressure indepen-

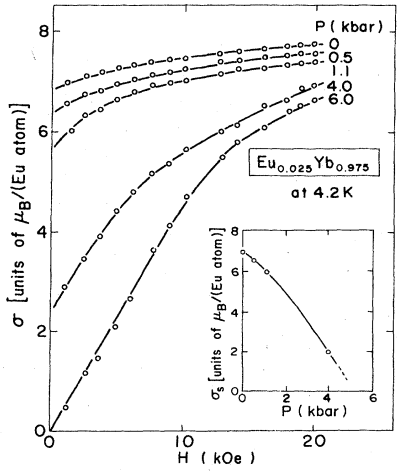

FIG. 8. Plots of magnetization σ [μ_B/(Eu atom)] at various pressures p as a function of effective field H. The inset shows spontaneous magnetization σ_s [μ_B/(Eu atom)] as a function of p. Temperature is 4.2 K and sample is $Eu_{0.025}Yb_{0.975}$.

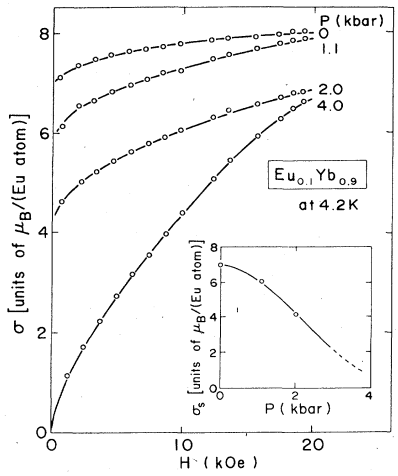

FIG. 9. Plots of magnetization σ [μ_B/(Eu atom)] at various pressures p as a function of effective field H. The inset shows spontaneous magnetization σ_s [μ_B/(Eu atom)] as a function of p. Temperature is 4.2 K and sample is $Eu_{0.10}Yb_{0.90}$.

dent. (c) All the σ_s versus p curves reveal that σ_s decreases with increasing pressure. Except for $x=0.025$, however, the curvatures of the curve are concave downwards and upwards in the low- and high-pressure ranges, respectively. For $x=0.025$, the T_c versus p curve has a maximum [Fig. 2(b)], while there is no maximum in the σ_s versus p curve. (d) From the smooth extrapolation of the σ_s versus p curve to $\sigma_s=0$, σ_s's for $x=0.025$, 0.1, and 0.2 samples vanish near $p=5$, 4.5, and 1.7 kbar, respectively. (e) Large field-induced magnetizations were observed at $p=6$ kbar in the paramagnetic region of $x=0.025$ and at $p=4$ kbar of $x=0.1$. (f) As is evident from Fig. 4(b), the sample of $x=0.2$ at 4.2 K exhibits spin-glass-like character above about $p=2$ kbar. In accordance with this fact, the σ versus H curve of $x=0.2$

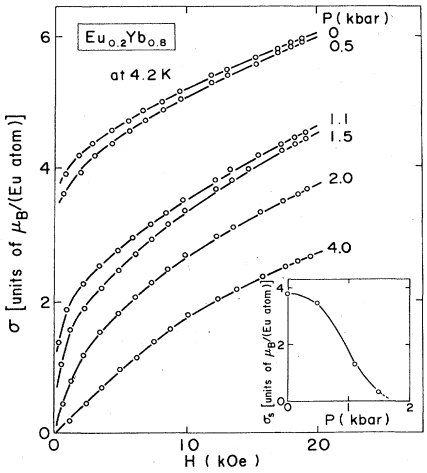

FIG. 10. Plots of magnetization σ [μ_B/(Eu atom)]] at various pressures p as a function of effective field H. The inset shows spontaneous magnetization σ_s [(μ_B/(Eu atom)] as a function of p. Temperature is 4.2 K and sample is $Eu_{0.20}Yb_{0.80}$.

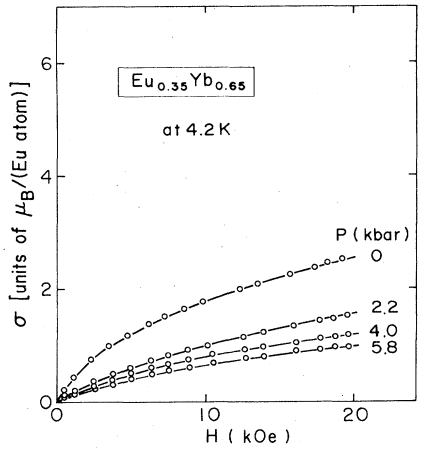

FIG. 11. Plots of magnetization σ [μ_B/(Eu atom)] at various pressures p as a function of effective field H. Temperature is 4.2 K and sample is $Eu_{0.35}Yb_{0.65}$.

shows no spontaneous magnetization above $p=2$ kbar. For $x=0.35$, $\partial M/\partial H$ decreases against the initial pressurization, but the rate of decrease becomes small with increasing pressure.

D. Pressure effect on the electrical resistivity

The resistivity measurements at high pressures were carried out for the alloys of $x=0.025$, which is the most dilute and shows only ferromagnetic character, and of $x=0.35$, which is relatively concentrated and shows only spin-glass-like character. In Figs. 12(a) and 12(b) are shown the ρ versus T curves for $x=0.025$ at various pressures, where the results up to 7.8 kbar and above are shown in Figs. 12(a) and 12(b), respectively. The break points indicated by arrows in the curves in the lower temperature range in Fig. 12(a) are the Curie temperatures T_c; T_c shifts to lower temperatures with increasing p and disappears in the curve at $p=6.4$ kbar. In the curve at $p=2.9$ kbar, on the other hand, a broad hump appears around $T=120$ K. The maximum of the hump shifts to lower temperatures as p increases, and it is around 60 K at $p=7.8$ kbar. Although the semiconducting character is seen in Fig. 12(a), the character becomes more definite when p increases, as seen in Fig. 12(b). In the inset of Fig. 12(b), the $\ln\rho$ versus T^{-1} plot at $p=14.9$ kbar is shown. From the plot, the energy gaps E of the semiconductor were evaluated to be 4.27×10^{-4} and 0.014 eV at low- and high-temperature ranges, respectively. The latter value is comparable with that of pure Yb obtained by McWhan *et al.*[7]

Figure 13 shows the ρ versus T curve of $x=0.35$ at various pressures. This sample is semiconducting at ambient pressure [Fig. 1(b)] and the character becomes clearer at higher pressures. From the slopes of the low- and high-temperature ranges of $\ln\rho$ versus T^{-1} plots at $p=14.6$ kbar shown in the inset of Fig. 13, the energy gaps E were evaluated to be 1.15×10^{-3} and 0.012 eV, respectively.

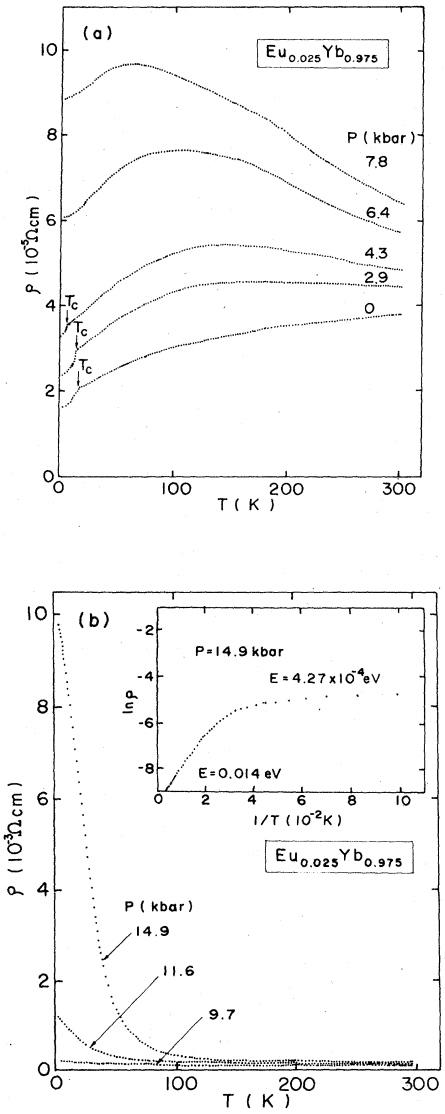

FIG. 12. (a) Electrical resistivity ρ vs temperature T curves at various pressures p up to 7.8 kbar and (b) above 9.7 kbar for $Eu_{0.025}Yb_{0.975}$. The inset shows $\ln\rho$ vs T^{-1} plot at 14.9 kbar.

E. Thermal expansion

Because of the remarkable negative pressure dependence of T_c, large positive spontaneous volume magnetostriction was expected to be observed in the thermal expansion below T_c. As the detailed results have been reported in our previous paper,[11] we will give a brief summary here. The spontaneous volume magnetostriction $\omega_s(T)$ is generally described as follows:[17]

$$\omega_s(T)=\kappa C M^2(T)\ , \tag{1}$$

where κ, C, and M are the volume compressibility, volume magnetostriction coupling constant, and magnetization, respectively. The value of $\omega_s(T)$ was derived by subtracting the phonon part from the observed result in the present alloy system, and the phonon part was

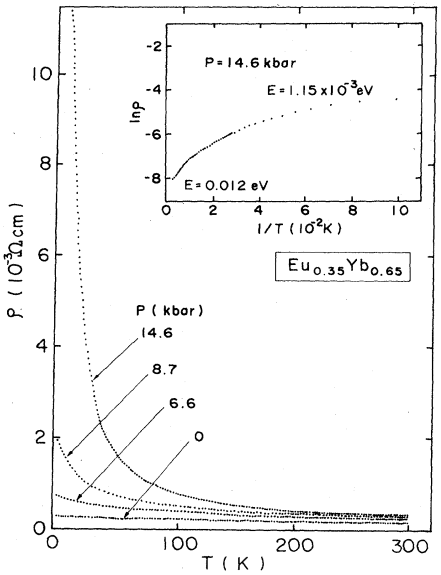

FIG. 13. Electrical resistivity ρ vs temperature T curve at various pressures p for $Eu_{0.35}Yb_{0.65}$. The inset shows $\ln\rho$ vs T^{-1} plot at 14.6 kbar.

evaluated from the thermal expansion of pure Yb. From Eq. (1), κC for $x=0.1$ and 0.2 are 4.8×10^{-8} and 4.2×10^{-8} cm^6/emu^2, respectively. These values are fairly large in comparison with those of well-known Invar alloys; for example, 0.9×10^{-8} cm^6/emu^2 for $Fe_{65}Ni_{35}$,[18] and 0.63×10^{-8} cm^6/emu^2 for $Fe_{75}Pt_{25}$,[18] respectively. Since κC is $1/4N^2\mu_B^2(\partial J/\partial\omega)$ on the basis of the localized electron model,[17] large κC and pressure dependence of T_c mean that the volume dependence of exchange constant J is very large.

IV. DISCUSSION

A. Change of the number of conduction electrons

It is well known that pure Yb, which is one of the constituents of the alloy system in the present work, is semimetallic at ambient pressure,[6] becomes semiconducting at high pressures above about 10 kbar, and then transforms into a metallic bcc phase near 40 kbar.[7] Rather detailed theoretical approaches have been used to study these interesting pressure-induced transformations in pure Yb. According to the volume-dependent band-structure calculation of Yb by Johansen and Mackintosh,[19] electron and hole pockets exist near L and many other symmetry points, respectively, at ambient pressure. They have also maintained, on the basis of their calculations, that the d-resonance broadening is induced with application of pressure, and resulting increase in sp-d hybridization at the Fermi level produces the band gap which is the cause of the transition to the semiconducting state. On the other hand, Koelling and Harmon[20] have pointed out that electron and hole pockets exist near the symmetry points K and W, respectively, and that the former are very sensitive to the crystal potential.

Jullien and Jerome[21] have estimated the number of conduction electrons in the electron pocket, using their data on the galvanomagnetic measurement for pure Yb, to be 0.02/(Yb atom) at ambient pressure. Therefore, the number of effective carriers n (electrons plus holes) was estimated as 0.04/(Yb atom), since Yb is semimetallic at ambient pressure. Then, n decreases linearly at a rate of $\Delta n/\Delta p = -0.04$ K/kbar as pressure increases and becomes zero around $p = 10$ kbar at a temperature of 4.2 K. As is evident from Figs. 12 and 13, it may be reasonably understood that we can discuss the pressure dependence of n in the present alloy system in a similar way to that in Yb.

The transition from the semimetallic to semiconducting states is induced also by the substitution of Eu for Yb (alloying effect) in the Eu-Yb alloy system near a Eu concentration x of 0.1 [Fig. 1(b)]. Therefore, both the application of pressure on pure Yb and the alloying effect in the Eu-Yb alloy system presently investigated may have similar effects on the electrical properties. In case of pressurization, the transition to the semiconducting state occurs through the deformation of the band resulting from the lattice or volume contraction. However, the alloying effect cannot be explained by the mechanism of Johansen and Mackintosh,[19] because the lattice constant increases with increasing x in the Eu_xYb_{1-x} system. In order to remove this inconsistency, therefore, one might propose that, in the alloying effect, the fictitious fcc Eu acts as insulator or semiconductor. Because of these circumstances, we will arrange and investigate the data obtained in the present work as a function not of the lattice constant but mainly of the number of carriers n which is controllable by both pressure p and concentration x.

B. Pressure-sensitive ferromagnetic state

On the basis of the free-electron model of the Ruderman-Kittel-Kasuya-Yosida (RKKY) interaction, T_c is expressed as follows:[2]

$$T_c = -\frac{3n^2J^2(g-1)^2j(j+1)}{kE_FV^2}\sum_{n\neq 0}F(2k_FR_{0n}) , \qquad (2)$$

where n, E_F, k_F, and $F(2k_FR_{0n})$ are the number of carriers (electrons plus holes), the Fermi energy, the Fermi wave vector, and the Friedel oscillation function, respectively. With this equation (2), Liu[4,22] studied the pressure effect on T_c of heavy rare-earth metals. In his first paper, he assumed that n and F are pressure independent, and in his second paper carried out the calculation using his estimated $5d\,6s$ band.

In the present alloy system, the number of carriers n decreases with increasing pressure, so that all the parameters n, E_F, k_F, and $F(2k_FR_{0n})$ in Eq. (3) have been considered to be pressure sensitive. The pressure dependence of the volume V was not taken into consideration, since the value of the volume compressibility, $V^{-1}\Delta V/\Delta p = -7.46\times 10^{-3}$ kbar^{-1},[23] is very small in comparison with the pressure coefficient of n, $n^{-1}\Delta n/\Delta p = -0.2$ kbar^{-1}.[21] In other words, this comparison means that it is not necessary to consider our data as a function of the lattice constant, as mentioned in Sec. II A.

For the pressure-sensitive factors in RKKY interaction, the following discussion will be made on the basis of Mattis's relation $T_c \sim k_F^4(\mathrm{WMF})$.[24] Then we get the following by simple differentiation with respect to p:

$$\frac{d\ln T_c}{dp} = \frac{d\ln[k_F^4(\mathrm{WMF})]}{dp}$$

$$= \frac{d\ln[k_F^4(\mathrm{WMF})]}{d\ln n}\frac{d\ln n}{dp} = \frac{d\ln n}{dp} , \qquad (3)$$

where the last equation was derived from the relation $k_F^4(\mathrm{WMF}) \propto n$ when the value of n is less than 0.15.[24] According to Eq. (3), the positive $\Delta T_c/\Delta p$ comes from the positive $\Delta n/\Delta p$. Therefore the positive $\Delta T_c/\Delta p$ for $x = 0.025$, at which concentration the alloy is semimetallic, in the lower-pressure range [Fig. 2(b)] could not be explained with Eq. (3), since we have assumed that n decreases with increasing p for this alloy as mentioned above. In order to remove this inconsistency, we have considered the following. We have already pointed out in Sec. III A that the large excess magnetic moment of $0.6\mu_B$/(Eu atom) at 0 K in comparison with the theoretically expected value may come from the polarization of the $5d\,6s$ band. In other words, the split of the band due to the exchange field will be realized. When pressure is applied, the semimetallic overlapping of the split band may increase due to the pressure-induced band widening, resulting in the increase of n and the positive $\Delta n/\Delta p$.

With further increase in p, the decrease of band polarization and sp-d hybridization tends to create the energy gap. In the semiconducting alloy for $x > 0.1$, it may be assumed that n in Eq. (3) is expressed as $n = n_0\exp(-E/kT)$ and that $\Delta T_c/\Delta p$ comes from the pressure effect on n through that on the energy gap E. Since E increases with the application of pressure, n is expected to decrease with p. From these arguments, the fact that T_c for $x = 0.025$ decreases rapidly above $p = 3$ kbar after reaching a maximum will be attributable to the strong pressure effect on n through E, since the alloy shows semiconducting character above $p = 3$ kbar as seen in Fig. 12(a). Although the pressure dependence of T_c for $x = 0.025$ could tentatively be understood in these ways, a detailed check should be required.

The large negative $\Delta T_c/\Delta p$ for $x = 0.1$ and 0.2, which are semiconducting means a drastic decrease in n with p and could be regarded as an indication of remarkable n-dependent volume magnetostriction below T_c. Positive volume magnetostriction in the present alloy system is, however, somewhat different in mechanism from that in the well-known Invar $3d$ metal alloys such as Fe-Ni and Fe-Pt. In the case of Invar alloys, the behavior is attributed to the volume dependence of the d band (the volume-induced band widening effect).[17] In the case of the Eu-Yb alloy system presently studied, on the other hand, the volume expands below T_c so as to induce a decrease in the band gap E and an increase in n, resulting in the decrease of the magnetic exchange energy (carrier number effect).

C. Spin-glass-like state

According to the simple RKKY model, the decrease in n changes the magnetic phase from ferromagnetic directly to the paramagnetic. In the Eu-Yb alloys with $x \geq 0.2$, however, the spin-glass-like phase appears at low temperatures [Fig. 1(a)]. This fact suggests that other kinds of interactions different from the RKKY type should also be considered in this concentration range. Furthermore, even if the remaining RKKY interaction will be suppressed with pressure, the spin-glass-like phase does not appear for the alloys of $x=0.025$ and 0.1. Therefore, another kind of interaction mentioned above may be the one which is effective for the appearance of the spin-glass-like phase for $x \geq 0.2$, but ineffective for $x < 0.2$. One of the key points in understanding these circumstances will be the fact that the concentration $x=0.2$ is very close to $x=0.195$, the fcc percolation limit.[25] Therefore, the other kind of interaction is likely to be of an antiferromagnetic short-range type, while the RKKY interaction is a long-range type. It has been pointed out that in the fcc crystal structure, the short-range antiferromagnetic interactions have frustration and high degeneracy in the magnetic structure.[26] However, the appearance of the spin-glass-like phase in the present alloys may be attributable to the heterogeneous distribution of interactions which is statistically unavoidable in the alloying process. A similar mechanism has been reported for the insulating spin-glass system of $Eu_xSr_{1-x}S$.[27]

Next, we will discuss the pressure effect on T_g and related problems. The long-range RKKY interaction still remains in the samples as mentioned above, and it produced ferromagnetic clusters which are distributed randomly due to the spatial fluctuation of the short-range interaction. Because of the pressure sensitive character of the RKKY interaction, the ferromagnetic clusters become vague, resulting in the decrease of T_g with initial application of pressure. But once the RKKY interaction becomes ineffective at large enough pressure, the pressure dependence of the short-range interaction dominates. The positive $\Delta T_g/\Delta p$ at relatively high pressures as seen in Fig. 6(b), for example, may come from this circumstance.

Since it may be assumed that the value of χ at T_g is roughly proportional to the size or the number of ferromagnetic clusters, the decrease in ferromagnetic clusters due to pressure will bring a strong negative pressure dependence of χ at T_g. On the basis of spin-glass theory,[28,29] T_g is expressed as $T_g \sim \sqrt{z}\,\Delta J$ where ΔJ is the standard deviation of the exchange interaction J. From the fact that the pressure dependence of T_g is considerably smaller in comparison with that of T_c, we can say that ΔJ is almost insensitive to pressure, contrary to the case of the RKKY interaction.

The reentrant phenomena (paramagnetic—ferromagnetic—spin-glass phases) shown in Fig. 1 have been found in many other systems. The examples are $Au_{1-x}Fe_x$ (Ref. 30), $(Pd, Fe)_{1-x}Mn_x$ (Refs. 16 and 31), $(Fe_{1-x}Mn_x)_{75}P_{16}B_6Al_3$ (Ref. 32), $(Fe_{1-x}Ni_x)_{75}P_{16}B_6Al_3$ (Ref. 32), and $Eu_{1-x}Sr_xS$ (Ref. 27). The first and second examples are crystallized $3d$-electron systems, the third and fourth are amorphous $3d$ electron systems, and the last one is an insulating rare-earth system. Furthermore, the system Eu_xYb_{1-x} presently employed is a semiconducting localized $4f$ electron system. The triple-point concentration, x_c reported are 0.16, 0.06, 0.40, and 0.83 for $Au_{1-x}Fe_x$, $(Pd_{0.9935}Fe_{0.0065})_{1-x}Mn_x$, $(Fe_{1-x}Mn_x)_{75}P_{16}B_6Al_3$, and $(Fe_{1-x}Ni_x)_{75}P_{16}B_6Al_3$, respectively. The magnetic properties under pressure which are common among these systems, are arranged as follows. (a) The signs of $\Delta T_c/\Delta p$ and $\Delta T_t/\Delta p$ for $x < x_c$ are negative and positive, respectively. (b) At $x \simeq x_c$, the χ versus T curve is asymmetric and the χ value near T_g drastically decreases with increasing pressure. (c) In some systems, the sign change in $\Delta T_g/\Delta p$ from negative to positive occurs as pressure increases. (d) The pressure dependence of the χ value at T_g is negative. These results are also maintained in a Eu-Yb system in the present work. Therefore it may safely be concluded that the response of the magnetism of the $5d\,6s$ band to pressure is very similar to that of the $3d$ band.

D. Resistivity maximum

As seen in Fig. 12(a), the resistivity ρ versus T curves for $x=0.025$ have maxima in the paramagnetic temperature range and the temperature at the maximum shifts to the lower-temperature side with increasing pressure. Up to $p=4.3$ kbar, the temperature dependences of the curves below T_c have been expressed experimentally as AT^{α}, where the α value increases from $\frac{3}{2}$ at 0 kbar to 2 at 4.3 kbar while A is almost constant. Furthermore, the curves at $p=6.4$ and 7.8 kbar below $T=30$ K are expressed as $AT^{3/2}$, where A at 7.8 kbar is larger than it is at 6.4 kbar.

Although they are not ferromagnetic cases, we will discuss the resistivity maxima of two examples: (i) a simple semiconductor, containing Bi impurity[33,34] and (ii) a spin-glass alloy, CuMn.[35] For (i), the electrical resistivity ρ is expressed as $\rho=(en\mu)^{-1}$, where e, n, and μ are the electron charge, the number of carriers, and the mobility, respectively. As temperature rises, μ decreases because of the increase of the phonon scattering and n increases by thermal excitation over a narrow energy gap. Then the maximum in the ρ versus T curve occurs as the result of the competition between these two causes. However, the temperature at which ρ reaches its maximum tends to shift to the higher-temperature side with increasing pressure, since the energy gap increases with increasing pressure. Therefore, this analysis is not applicable to the present result.

In the case of (ii), on the other hand, Ford and Mydosh[35] have interpreted the maximum as arising from the competition between the creation of short-range magnetic ordering at temperatures far beyond T_g and the Kondo effect. There, on the basis of the conduction-electron scattering by a magnetic impurity, ρ was expressed $\rho=\rho_0+AT^{3/2}$, where the symbols in the equations are from their paper, Ref. 35. According to their analysis, the present results obtained for $p=6.4$ and 7.8 kbar are likely to be understood qualitatively by taking the thermal excitation over energy gap into consideration, instead of the Kondo effect. Then the carrier number decreases, as temperature decreases, due to the decrease of thermal excitations over energy gap, and ρ increases in the high-

temperature side. When the temperature decreases further, short-range magnetic ordering develops dominantly, or overcomes the effect of thermal excitation, and tends to decrease after reaching a maximum. As pressure increases, the RKKY interaction for the short-range magnetic ordering becomes weak and the temperature at which ρ reaches its maximum falls. Concerning the increase of A with increasing pressure, it may be roughly understood that A will be inversely proportional to n, $A \propto n^{-1}$.[35]

ACKNOWLEDGMENTS

The authors wish to express their thanks to Mr. Kurisu, Mr. Suenaga, and Mr. Masumoto for their experimental assistance. One of us (H.F.) wishes to express his thanks for financial aid from the Japanese Ministry of Education, Science and Culture.

[1]R. J. Elliott, *Magnetic Properties of Rare Earth Metals* (Plenum, New York, 1972).
[2]A. J. Dekker, J. Appl. Phys. **36**, 906 (1965).
[3]K. H. J. Buschow, Rep. Prog. Phys. **42**, 1373 (1979).
[4]G. S. Fleming and S. H. Liu, Phys. Rev. B **2**, 164 (1970).
[5]W. G. Moffatt, *The Handbook of Binary Phase Diagrams* (General Electric Corp., New York, 1978).
[6]W. R. Datars and S. Tanuma, Phys. Lett. B **27**, 182 (1968).
[7]D. B. McWhan, T. M. Rice, and P. H. Schmidt, Phys. Rev. **177**, 1063 (1969).
[8]E. King and I. R. Harris, J. Less-Common Met. **20**, 237 (1970).
[9]H. Kadomatsu, T. Tsutaoka, and H. Fujiwara, J. Phys. Soc. Jpn. **53**, 3153 (1984).
[10]H. Kadomatsu, T. Tsutaoka, and H. Fujiwara, J. Phys. Soc. Jpn. **53**, 3751 (1984).
[11]H. Kadomatsu, T. Tsutaoka, and H. Fujiwara, J. Phys. Soc. Jpn. **53**, 4106 (1984).
[12]H. Fujiwara,H. Kadomatsu, and K. Tohma, Rev. Sci. Instrum. **51**, 1345 (1980).
[13]H. Kadomatsu, K. Tohma, M. Kurisu, and H. Fujiwara, Jpn. J. Appl. Phys. **21**, 140 (1982).
[14]K. H. Unterreiner and B. Elschner, Z. Angew. Phys. **30**, 239 (1970); S. Legvold and J. P. Beaver, Solid State Commun. **31**, 727 (1979); S. Legvold, *Ferromagnetic Materials*, edited by E. P. Wohlfarth (North-Holland, New York, 1980), Vol. 1, Chap. 3, p. 184.
[15]H. Fujiwara, H. Kadomatsu, K. Ohishi, and Y. Yamamoto, J. Phys. Soc. Jpn. **40**, 1010 (1976).
[16]B. H. Verbeek, G. J. Nieuwenhuys, H. Stocker, and J. A. Mydosh, Phys. Rev. Lett. **40**, 586 (1978).
[17]M. Shiga, J. Phys. Soc. Jpn. **50**, 2573 (1981).
[18]Y. Nakamura, K. Sumiyama, and M. Shiga, J. Magn. Magn. Mater. **12**, 127 (1979).
[19]G. Johansen and A. R. Mackintosh, Solid State Commun. **8**, 121 (1970).
[20]D. D. Koelling and B. N. Harmon, Bull. Am. Phys. Soc. **17**, 94 (1972).
[21]R. Jullien and D. Jerome, J. Phys. Chem. Solids **32**, 257 (1971).
[22]S. H. Liu, Phys. Rev. **127**, 1889 (1962).
[23]P. W. Bridgman, *Collected Experimental Papers* (Harvard University Press, Cambridge, Mass., 1984), Vol. VII, p. 4323.
[24]D. C. Mattis, *Theory of Magnetism* (Harper and Row, New York, 1965), p. 195.
[25]J. W. Essam, *Phase Transitions and Critical Phenomena*, edited by C. Domb and M. S. Green (Academic, London, 1972), p. 197.
[26]J. Villain, Z. Phys. B **33**, 31 (1979).
[27]H. Maletta and W. Felsch, Phys. Rev. B **20**, 1245 (1979).
[28]S. F. Edwards and P. W. Anderson, J. Phys. F **5**, 965 (1975).
[29]D. Sherrington and S. Kirkpatrick, Phys. Rev. Lett. **35**, 1792 (1975).
[30]J. A. Mydosh, P. J. Ford, M. P. Kawatra, and T. E. Whall, Phys. Rev. B **10**, 2845 (1974).
[31]M. K. Wu, R. G. Aitken, C. W. Chu, C. Y. Huang, and C. E. Olsen, J. Appl. Phys. **50**, 7356 (1979).
[32]C. W. Chu, M. K. Wu, B. J. Jin, W. Y. Lai, and H. S. Chen, Phys. Rev. Lett. **46**, 1643 (1981).
[33]N. Thompson and H. H. Wills, Proc. R. Soc. London, Ser. A **155**, 111 (1936).
[34]A. H. Wilson, *The Theory of Metals* (Cambridge University Press, Cambridge, England, 1965), p. 227.
[35]P. J. Ford and J. A. Mydosh, Phys. Rev. **14**, 2057 (1976).